PCCP

Physical Chemistry Chemical Physics

This paper is published as part of a PCCP Themed Issue on:

Interfacial Systems Chemistry: Out of the Vacuum, Through the Liquid, Into the Cell

Guest Editors: Professor Armin Gölzhäuser (Bielefeld) & Professor Christof Wöll (Karlsruhe)

Self-assembled monolayers of benzylmercaptan and *para*-cyanobenzylmercaptan on gold: surface infrared spectroscopic characterization
K. Rajalingam, L. Hallmann, T. Strunskus, A. Bashir, C. Wöll and F. Tuczek, *Phys. Chem. Chem. Phys.*, 2010
DOI: 10.1039/b923628g

The formation of nitrogen-containing functional groups on carbon nanotube surfaces: a quantitative XPS and TPD study
Shankhamala Kundu, Wei Xia, Wilma Busser, Michael Becker, Diedrich A. Schmidt, Martina Havenith and Martin Muhler, *Phys. Chem. Chem. Phys.*, 2010
DOI: 10.1039/b923651a

Geometric and electronic structure of Pd/4-aminothiophenol/Au(111) metal–molecule–metal contacts: a periodic DFT study
Jan Kučera and Axel Groß, *Phys. Chem. Chem. Phys.*, 2010
DOI: 10.1039/b923700c

Ultrathin conductive carbon nanomembranes as support films for structural analysis of biological specimens
Daniel Rhinow, Janet Vonck, Michael Schranz, Andre Beyer, Armin Gölzhäuser and Norbert Hampp, *Phys. Chem. Chem. Phys.*, 2010
DOI: 10.1039/b923756a

Microstructured poly(2-oxazoline) bottle-brush brushes on nanocrystalline diamond
Naima A. Hutter, Andreas Reitinger, Ning Zhang, Marin Steenackers, Oliver A. Williams, Jose A. Garrido and Rainer Jordan, *Phys. Chem. Chem. Phys.*, 2010
DOI: 10.1039/b923789p

Model non-equilibrium molecular dynamics simulations of heat transfer from a hot gold surface to an alkylthiolate self-assembled monolayer
Yue Zhang, George L. Barnes, Tianying Yan and William L. Hase, *Phys. Chem. Chem. Phys.*, 2010
DOI: 10.1039/b923858c

Holey nanosheets by patterning with UV/ozone
Christoph T. Nottbohm, Sebastian Wiegmann, André Beyer and Armin Gölzhäuser, *Phys. Chem. Chem. Phys.*, 2010
DOI: 10.1039/b923863h

Tuning the local frictional and electrostatic responses of nanostructured $SrTiO_3$—surfaces by self-assembled molecular monolayers
Markos Paradinas, Luis Garzón, Florencio Sánchez, Romain Bachelet, David B. Amabilino, Josep Fontcuberta and Carmen Ocal, *Phys. Chem. Chem. Phys.*, 2010
DOI: 10.1039/b924227a

Influence of OH groups on charge transport across organic–organic interfaces: a systematic approach employing an "ideal" device
Zhi-Hong Wang, Daniel Käfer, Asif Bashir, Jan Götzen, Alexander Birkner, Gregor Witte and Christof Wöll, *Phys. Chem. Chem. Phys.*, 2010
DOI: 10.1039/b924230a

A combinatorial approach toward fabrication of surface-adsorbed metal nanoparticles for investigation of an enzyme reaction
H. Takei and T. Yamaguchi, *Phys. Chem. Chem. Phys.*, 2010
DOI: 10.1039/b924233n

Structural characterization of self-assembled monolayers of pyridine-terminated thiolates on gold
Jinxuan Liu, Björn Schüpbach, Asif Bashir, Osama Shekhah, Alexei Nefedov, Martin Kind, Andreas Terfort and Christof Wöll, *Phys. Chem. Chem. Phys.*, 2010
DOI: 10.1039/b924246p

Quantification of the adhesion strength of fibroblast cells on ethylene glycol terminated self-assembled monolayers by a microfluidic shear force assay
Christof Christophis, Michael Grunze and Axel Rosenhahn, *Phys. Chem. Chem. Phys.*, 2010
DOI: 10.1039/b924304f

Lipid coated mesoporous silica nanoparticles as photosensitive drug carriers
Yang Yang, Weixing Song, Anhe Wang, Pengli Zhu, Jinbo Fei and Junbai Li, *Phys. Chem. Chem. Phys.*, 2010
DOI: 10.1039/b924370d

On the electronic and geometrical structure of the *trans*- and *cis*-isomer of tetra-*tert*-butyl-azobenzene on Au(111)
Roland Schmidt, Sebastian Hagen, Daniel Brete, Robert Carley, Cornelius Gahl, Jadranka Dokić, Peter Saalfrank, Stefan Hecht, Petra Tegeder and Martin Weinelt, *Phys. Chem. Chem. Phys.*, 2010
DOI: 10.1039/b924409c

Oriented growth of the functionalized metal–organic framework CAU-1 on –OH- and –COOH-terminated self-assembled monolayers
Florian Hinterholzinger, Camilla Scherb, Tim Ahnfeldt, Norbert Stock and Thomas Bein, *Phys. Chem. Chem. Phys.*, 2010
DOI: 10.1039/b924657f

Interfacial coordination interactions studied on cobalt octaethylporphyrin and cobalt tetraphenylporphyrin monolayers on Au(111)
Yun Bai, Michael Sekita, Martin Schmid, Thomas Bischof, Hans-Peter Steinrück and J. Michael Gottfried, *Phys. Chem. Chem. Phys.*, 2010
DOI: 10.1039/b924974p

Probing adsorption and aggregation of insulin at a poly(acrylic acid) brush
Florian Evers, Christian Reichhart, Roland Steitz, Metin Tolan and Claus Czeslik, *Phys. Chem. Chem. Phys.*, 2010
DOI: 10.1039/b925134k

Nanocomposite microstructures with tunable mechanical and chemical properties
Sameh Tawfick, Xiaopei Deng, A. John Hart and Joerg Lahann, *Phys. Chem. Chem. Phys.*, 2010
DOI: 10.1039/c000304m

Self-assembly of triazatriangulenium-based functional adlayers on Au(111) surfaces

Sonja Kuhn,[a] Belinda Baisch,[a] Ulrich Jung,[a] Torben Johannsen,[a] Jens Kubitschke,[b] Rainer Herges*[b] and Olaf Magnussen*[a]

Received 2nd November 2009, Accepted 8th February 2010
First published as an Advance Article on the web 15th March 2010
DOI: 10.1039/b922882a

Detailed scanning tunneling microscopy studies of the attachment of freestanding molecular functions to Au(111) surfaces *via* self-assembly of functional molecules based on triazatriangulenium platforms are presented. As shown for molecules with side chains of different length and phenyl, azobenzyl, or azobenzyl derivatives with different terminal groups (iodo, cyano, or dimethyl) as functional units, this approach allows the preparation of very stable, hexagonally ordered adlayers. The intermolecular spacings in these adlayers are independent of the attached functions with the latter being orientated perpendicular to the Au surface. Due to their open structure, adlayers of platforms with attached functional groups exhibit a tendency towards bilayer formation, which can be suppressed by derivatization with appropriate terminal groups.

1. Introduction

The controlled attachment of organic molecules to metal surfaces is of major interest for preparation of functionalized surfaces and nanosystems.[1,2] Self-assembly at the metal/solution interface is widely used for this purpose.[3,4] Typically, this method utilizes the lateral interactions between the adsorbed molecules, which favor ordered, close-packed molecular layers, as *e.g.* in the prototypical case of thiol self-assembled monolayers on Au surfaces. By chemical modification of the molecules, such as derivatization of the end groups, a broad variety of chemical functionalities can be attached to the surface. However, for more complex functions, as for example photoswitchable moieties, this simple approach is only of limited use. In particular, preservation of such advanced molecular functions in adsorbed layers often requires a sufficiently large free volume,[5,6] *e.g.* to allow conformational changes, as well as the electronic decoupling of the functional units from the substrate.[7] This is most commonly accomplished by employing mixed monolayers with short-chain spacer molecules.[5,6,8–17] More modern approaches to enforce a sufficient free volume employ specially designed molecules, which feature additional bulky spacer groups[6,18–21] or molecular tripods[22–25] as basis. Nevertheless, these types of adlayers also exhibit intrinsic disadvantages such as a comparable low structural order or lack of temporal stability due to phase separation.

Adlayers with a much higher degree of order can be formed on metal surfaces by self-assembly of planar heterocyclic compounds, such as porphyrins or phthalocyanines.[26,27] These molecules adopt a planar adsorption geometry with intermolecular distances in the range of 1–2 nm, which can be controlled by the molecular structure. However, contrary to thiol-bound species they cannot be easily functionalized in a way that allows to mount functional groups perpendicular to the surface. In our previous publication we recently demonstrated a novel concept for attaching molecular functions to metal surfaces that combines the advantages of both approaches.[28] This new approach employs customizable molecular platforms based on the triazatriangulenium (TATA) ion (Fig. 1), which allows covalent attachment of a functional group to the central carbon atom. The platforms adsorb on the surface, acting as pedestals, which enforce a controlled orientation and distance of the functional groups with respect to the substrate surface. The spacing between the functions can be controlled by the lateral dimensions of the platforms, which depend on the length of the side chains attached to the nitrogen atoms of the TATA unit.

In this work, we report an in-depth structural study of TATA molecules on Au(111) by scanning tunneling microscopy (STM), covering a much larger range of different functional groups. First, the adlayer structure of the bare TATA platforms as well as their stability under various conditions including electrochemical environment will be discussed. Then we will focus on the structure of adlayers formed by platforms that are functionalized by phenyl, azobenzyl, or azobenzyl derivatives. Specifically, systematic studies on the influence of the conditions employed for the adlayer self-assembly (concentration, immersion time, temperature) and of the head groups of the attached functional units will be reported. We will show that by optimization of the molecular design and adlayer preparation well-defined, highly ordered functionalized monolayers can be prepared.

[a] *Institut für Experimentelle und Angewandte Physik, Christian-Albrechts-Universität zu Kiel, Leibnizstr. 19, 24118 Kiel, Germany. E-mail: magnussen@physik.uni-kiel.de*
[b] *Otto-Diels-Institut für Organische Chemie, Christian-Albrechts-Universität zu Kiel, Otto-Hahn-Platz 4, 24098 Kiel, Germany. E-mail: rherges@oc.uni-kiel.de*

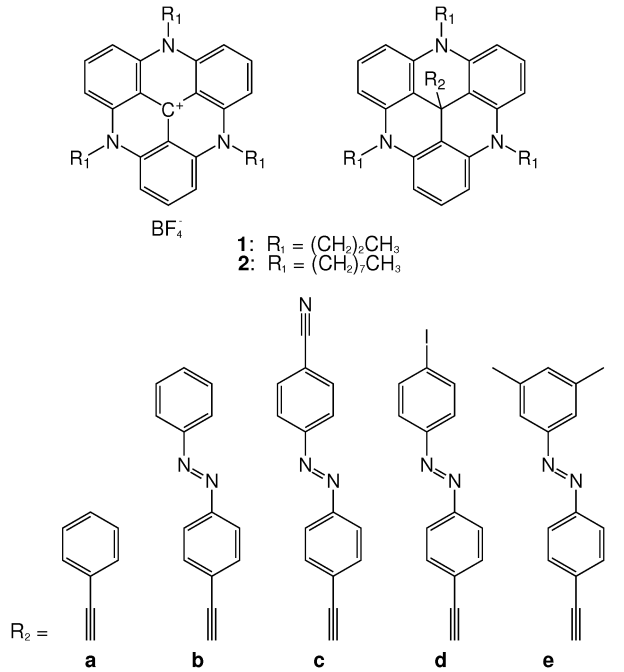

Fig. 1 Chemical structures of the TATA molecules used for preparation of self-assembled adlayers on Au(111).

2. Experimental

2.1 Materials

The TATA molecules used for preparation of the adlayers are shown in Fig. 1. The substances were synthesized following the procedure described in our previous paper.[28] The quality of all substances was verified by NMR and mass spectroscopy, indicating a purity better than 99%.

Au(111) single crystals with surface diameters of 10 mm, which were oriented within 0.3° (MaTecK GmbH, Jülich, Germany) were employed as substrates. Prior to usage, the crystals were cleaned by electrooxidation in 0.1 M H_2SO_4 and subsequent 4 min immersion into 0.1 M HCl. Then, the crystals were annealed in a butane gas flame for 2–5 min. To prepare the self-assembled layers the cleaned substrates were immersed into solutions of the TATA molecules in ethanol or toluene (Merck, p.a.) with concentrations of 5×10^{-7} to 1×10^{-3} M for periods of 30 min up to 48 h. Usually, the preparation was performed at room temperature, but in some experiments the solutions were kept at elevated temperatures (30, 40, 50, or 80 °C) during immersion to increase the surface mobility of the adsorbate molecules. After this, excess TATA molecules were removed by immersing the adlayer-modified substrates for several seconds to 30 min into the pure solvent, which was again heated in some experiments during immersion. Finally, the samples were dried in air and immediately transferred into the STM.

2.2 Instrumentation

For the STM measurements a PicoPlus SPM (Agilent, Inc., Santa Clara, USA) was employed. If not mentioned otherwise in the text, the measurements were carried out in air using mechanically cut Pt/Ir (70 : 30%) tips. In addition, *in situ* STM studies in electrochemical environment were performed in 0.1 M H_2SO_4 (Merck, suprapure) using electrochemically etched W tips with apiezon or polyethylene coating and Pt counter and reference electrodes. All potentials are given *versus* the saturated calomel electrode (SCE). The experiments were performed in constant current mode at tunneling currents ranging from 10 to 500 pA and bias voltages from 100 to 900 mV. The lateral drift in the STM images was corrected using a dedicated software.

3. Results and discussion

We first describe the adsorption of the pure triazatriangulenium cations **1** and **2**, *i.e.*, the bare molecular platforms, on the Au(111) surface. As shown in our previous publication[28] and illustrated in Fig. 2a–d these molecules form hexagonally ordered adlayers, indicative of a planar adsorption geometry. The lattice constant depends on the length of the side chains attached to the nitrogen atoms of the TATA platform and increases from 10.7 Å for propyl (**1**) to 12.6 Å for octyl (**2**) side chains (see also Table 1). Hence, the surface density of these molecules can be controlled by their molecular architecture, *i.e.*, the length of the alkyl side chains. Two rotational domains are visible, indicating a well-defined epitaxial relationship between adlayer and substrate lattice. The typical domain size ranges from several 10 up to more than 100 nm and was rather independent of the preparation conditions.

These structural data are in good agreement with simple commensurate superstructures, specifically a $(\sqrt{13} \times \sqrt{13})-$R13.9° for **1** adlayers and a $(\sqrt{19} \times \sqrt{19}) -$ R23.4° superstructure for **2** adlayers (Fig. 2e and f). Both the intermolecular distances (10.7 and 12.6 Å) as well as the angles between rotational domains in these structures match the experimental values within the error of the STM measurements. The packing density in these superstructures is surprisingly high and, in particular, incompatible with a complete planar orientation of the full molecule, *i.e.*, the TATA unit and the alkyl side chains. Consequently, the latter have to be partially tilted away from the Au surface. The commensurate nature of the superstructures and the high adlayer packing densities suggest that the TATA platforms are not only bound *via* van-der-Waals forces and interactions between the π electron system and the metal substrate, but also *via* more local bonds, presumably involving the nitrogen atoms of the molecule. The distance between these nitrogen atoms within the TATA entity (4.8 Å) is almost twice the nearest neighbor spacing of the Au(111) substrate atoms, allowing an adsorption geometry where all nitrogen atoms reside on identical sites of the Au lattice, binding to the surface *via* their lone electron pair. The latter would also explain the partial orientation of the alkyl side chains away from the surface as a consequence of the tetragonal coordination of the nitrogen atoms. For this TATA adsorption geometry a uniform molecular orientation results, where the vertices of the molecular platforms (*i.e.*, the benzene rings) point roughly towards the centers of the sides of three neighboring molecules. This type of arrangement indeed seems to be supported by high-resolution images of these adlayers.[28]

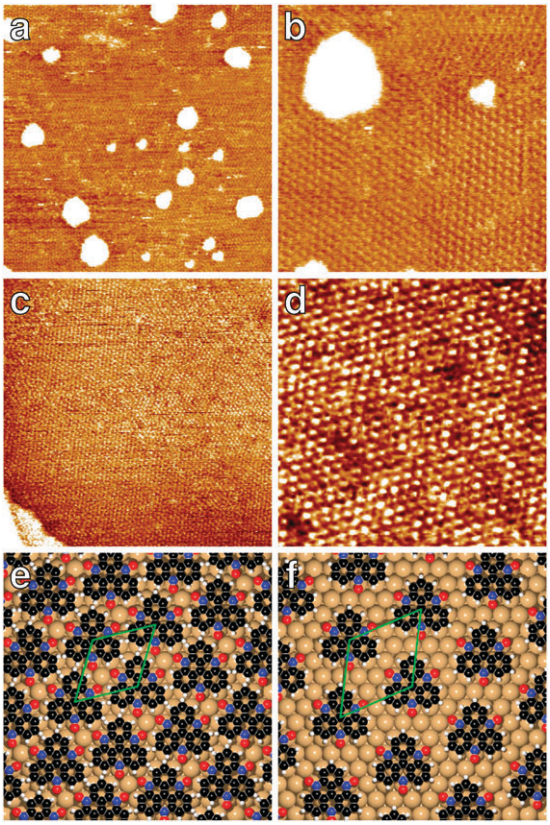

Fig. 2 (a, b) *In situ* STM images of an **1** adlayer on Au(111) in 0.1 M H_2SO_4 at 0.16 V. (a) Large scale topography (80 × 80 nm^2), (b) two rotational domains of the ordered adlayer structure (30 × 30 nm^2). (c, d) STM images of a **2** adlayer on Au(111), (c) 80 × 80 nm^2, (d) 30 × 30 nm^2. (e, f) Schematic models showing (e) the $(\sqrt{13} \times \sqrt{13}) - R13.9°$ superstructure of the **1** adlayer and (f) $(\sqrt{19} \times \sqrt{19}) - R23.4°$ superstructure of the **2** adlayer on Au(111). The alkyl side chains of the molecules are omitted in these models.

Table 1 Lattice parameters for TATA adlayers on Au(111)

Substance	Side chain	Functional group	a/Å	γ/°
1	Propyl		10.7 ± 0.2	59.2 ± 1.1
1a	Propyl	Phenyl	10.7 ± 0.9	59.1 ± 3.4
1b	Propyl	Azobenzyl	11.7 ± 0.8	60.0 ± 3.1
2	Octyl		12.6 ± 0.4	60.0 ± 2.9
2a	Octyl	Phenyl	12.6 ± 0.5	60.0 ± 3.0
2b	Octyl	Azobenzyl	12.5 ± 0.1	60.2 ± 0.6
2c	Octyl	Cyano azobenzyl	12.0 ± 0.1	60.0 ± 4.8
2d	Octyl	Iodo azobenzyl	12.7 ± 0.5	60.0 ± 3.6

As seen in larger scale images (Fig. 2a and c) the topography of Au(111) surfaces covered by **1** and **2** adlayers is similar to that of the bare substrate, exhibiting extended atomically smooth terraces separated by monoatomic steps. Hence, in contrast to thiols,[29] the formation of the TATA adlayers does not have a major effect on the Au surface morphology. In some cases Au monolayer islands with step heights of ≈ 2.35 Å are visible (Fig. 2a and b), which most likely results from release of additional Au atoms onto the surface, caused by lifting of the Au(111) herringbone reconstruction during the sample preparation.[30,31] Interestingly, TATA adsorption itself does not necessarily induce this lifting, however

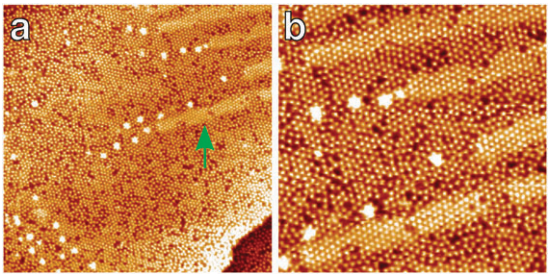

Fig. 3 STM images of a **2a** adlayer on Au(111) showing (a) dislocation lines of the Au surface reconstruction in parts of the imaged sample area (100 × 100 nm^2, reconstruction indicated by arrow) and (b) the enhanced packing density on top of the reconstructed surface areas (50 × 50 nm^2). In addition, small Au islands (white areas) are visible, resulting from the lifting of this metastable reconstruction.

occasionally (metastable) remnants of the characteristic double stripe network of the Au reconstruction can still be seen underneath the TATA adlayer (Fig. 3a). In these areas the adlayer packing density is roughly 4% enhanced (Fig. 3b), in agreement with a commensurate arrangement on the more densely packed reconstructed surface. This again supports the proposed local binding of TATA to the metal surface. Furthermore, the orientation of these double stripes relative to the TATA adlattice confirms the proposed epitaxial relationship.

The observed molecular structures and the adlayer morphology (*e.g.* domain size, defect density) did not vary significantly with time during the STM measurements. Even after three days in air the same ordered adlayers could still be observed. Additional SPR experiments[32] revealed that the adlayers were stable in different solvents (ethanol, dichloromethane, toluene). Moreover, the TATA layers were stable in aqueous solutions of various pHs (0.1 M H_2SO_4, and 0.1 M $NaClO_4$ with Britton-Robinson buffer at pH = 5 to 7). Electrochemical studies of Au(111) single crystal electrodes covered with **1** and **1b** adlayers were performed by cyclic voltammetry in 0.1 M H_2SO_4, aiming to clarify the stability of these adlayers. As an example, Fig. 4a shows a voltammogram of a **1** adlayer (black line), which revealed a distinctly different behavior than clean Au(111) electrodes. Specifically, a sharp anodic peak at 0.75 V and a corresponding broader cathodic feature centered around 0.65 V was found. The charge density of the anodic peak of (9.7 ± 2.5) μC cm^{-2} is smaller than the value expected for a one-electron transfer reaction. These cyclic voltammograms were stable in successive cycles, indicating that the adlayer is not irreversibly desorbed or oxidized, although reversible desorption/readsorption cannot be excluded. Furthermore, lowering the potential down to the onset of hydrogen evolution (−0.4 V) resulted in similar voltammograms, indicating that the adlayers are also stable at negative potentials. More detailed electrochemical studies are currently in progress. *In situ* STM studies of **1** adlayers in the electrochemical environment (Fig. 4b–e), in which the potential was first stepwise increased from 0.16 to 0.64 V and then decreased to 0.43 V again, show that the adlayer superstructure is present. Only the quality of the STM images deteriorates at more positive potentials, which may be

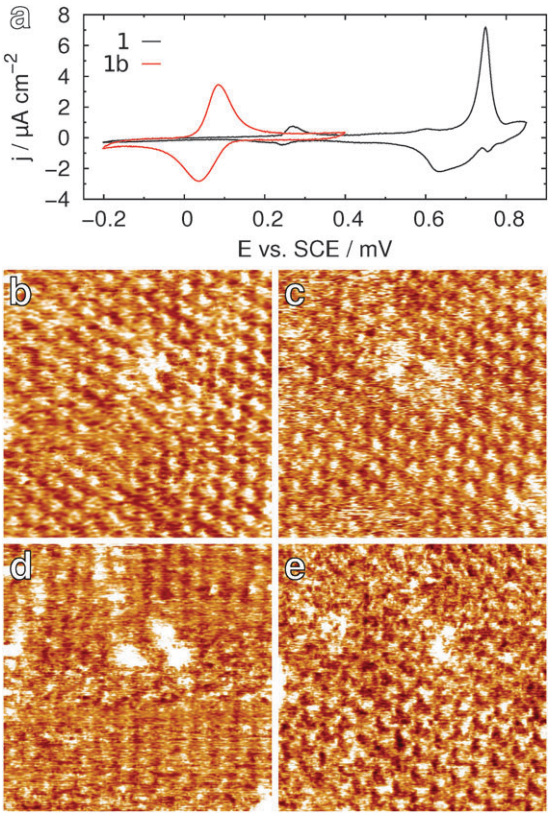

Fig. 4 (a) Cyclic voltammograms of a **1** and a **1b** adlayer on Au(111) in 0.1 M H_2SO_4 at a scan rate of 20 mV s^{-1}. (b–e) Selected *in situ* STM images (12.5 × 12.5 nm^2) of a sequence showing a **1** adlayer on Au(111) in 0.1 M H_2SO_4 at (b) 0.16, (c) 0.27, (d) 0.64, and (e) 0.43 V.

related to the different tunneling parameters in this regime. Furthermore, no change in the lattice parameters could be detected within the experimental precision of the STM measurements. Consequently, these adsorbates are stable on the surface over a wide potential range between the onset of hydrogen evolution and potentials close to the onset of Au surface oxidation.

Having described the adsorption behavior of the pure triazatriangulenium platform, we will now address the case of TATA molecules with a functional group attached to the central carbon atom. In our previous paper we demonstrated for selected molecules of this type (**1a**, **1b**, and **2a**) the formation of similar hexagonally ordered adlayers as for the pure TATA cations.[28] More systematic studies, covering a variety of functional moieties, which were all connected to the platform *via* an ethinyl spacer group, show this to be generally true for adlayers of these substances on Au(111). As can be clearly observed in the STM images in Fig. 5, the characteristic hexagonal superstructure with distances in the range of 1 nm is formed by all studied molecules, independent of the central functional group. This strongly suggests an identical adsorption geometry, *i.e.*, a surface-parallel adsorption of the TATA platforms with the alkyl side chains partially tilted upwards and the functional group oriented perpendicular to the surface. Although the central functional groups could not be imaged directly in the STM experiments, this geometry is also supported by the dependence of the image quality on the tunneling conditions. Specifically, as expected for a vertical orientation of the functional group, stable imaging of molecules with larger functional units is only possible at considerably larger tunneling gap widths: while the adlattice of the pure TATA platform could be clearly resolved even at tunneling currents of 900 pA, molecular resolution images of platforms with attached azobenzyl groups (height ≈ 17 Å) required currents of <100 pA. Clear proof that the molecules adsorb intact on the surface with the central group remaining attached comes from electrochemical investigations of **1b** and **2b** modified Au(111) electrodes in 0.1 M H_2SO_4, which show the characteristic redox peaks of the azobenzene moiety at ≈0.06 V (Fig. 4a), as well as from various spectroscopic studies, which will be subject of a forthcoming paper.

The lattice parameters of the adlayers formed by the functionalized platforms are summarized in Table 1. In most cases, the observed lattice spacing is very similar to that found for the corresponding bare TATA molecules, indicating that the lateral spacings of the molecules are dominated by the bulkier platforms rather than by the attached functional groups. Only for the molecules with propyl side chains and azobenzene as functional group (**1b**) a noticeable difference was found. However, this may be related to the small domain size in this adlayer (see below) and the resulting large error in determining the intermolecular spacings. The average domain sizes are usually smaller than for the bare TATA platforms, although they typically exceed several 10 nm. In addition, in some areas a more disordered adlayer with only short range order (but very similar intermolecular spacings) is observed.

STM images of adlayers formed by the functionalized TATA platforms exhibit a characteristic two-level structure with irregularly shaped islands (or holes) that usually differ by ≈4 Å in apparent height. However, in rare cases dramatic changes in the apparent height of these structures were observed after spontaneous jumps in the state of the tunneling tip. An example is shown in Fig. 6a, where for a **1b** adlayer reversible changes (indicated by arrows) between an imaging state with the typical island height of ≈4 Å and one with a much lower height of ≈1.5 Å are visible (Fig. 6b). The clear difference in height from that of monoatomic Au steps and the strong dependence on the tip state indicates that these features are not related to structural defects in the Au substrate, such as monolayer islands or pits, but have to be caused by local differences in the adsorbed molecular layer. On both height levels the same hexagonal superstructure is visible, indicating that the molecular adlayer is present on the surface in the darker (*i.e.*, lower) as well as the brighter (*i.e.*, higher) appearing areas and exhibits in both identical lattice parameters (Fig. 6c). Extrapolation of the superstructure lattice observed in the lower level surface areas into the areas covered by the higher level structure suggests that the adlattices in both areas are either not or only slightly shifted with respect to each other.

We attribute these observations to the formation of a mixed monolayer/bilayer phase during the self-assembly. Here the darker areas correspond to a single molecular layer, with the functional unit pointing away from the surface, and the brighter ones to an interdigitated bilayer structure, formed by

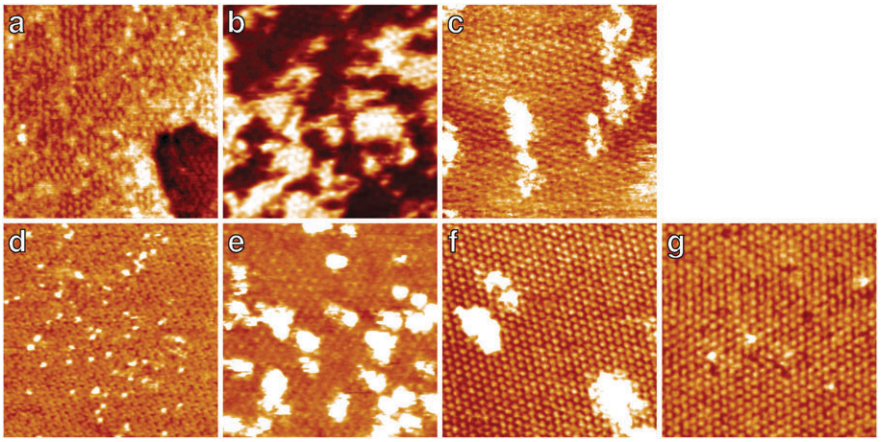

Fig. 5 STM images (30 × 30 nm^2) of various functionalized TATA adlayers on Au(111): (a) **1a**, (b) **1b**, (c) **1e**, (d) **2a**, (e) **2b**, (f) **2c**, and (g) **2d**.

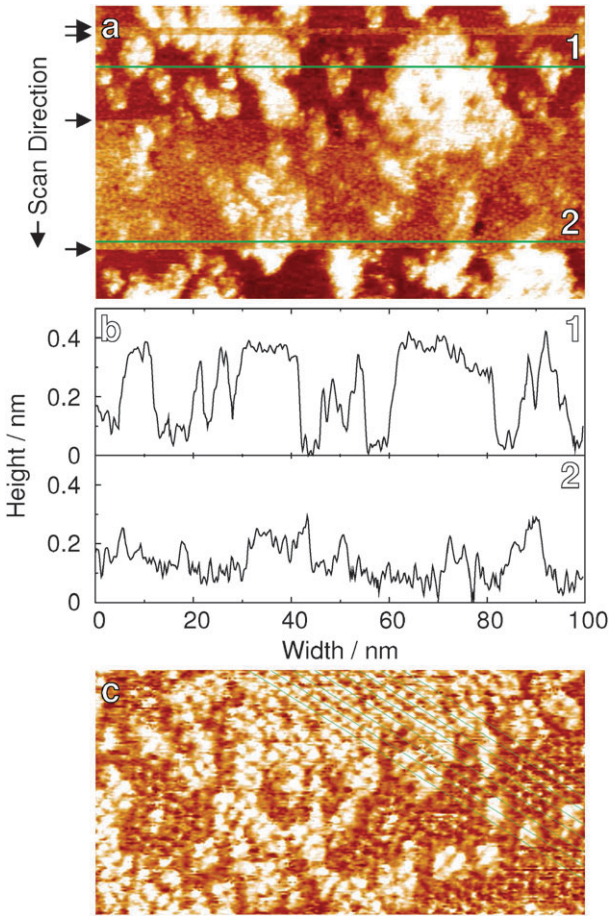

Fig. 6 (a) Effect of the tip state on STM images for a **1b** adlayer (100 × 60 nm^2, I_T = 10 pA, U_{bias} = 0.78 V). Spontaneous changes in the tip state are indicated by arrows. (b) Height profiles obtained at the positions indicated in (a). (c) STM image of a **2b** adlayer showing the adlattice in mono- and bilayer areas (50 × 25 nm^2).

adsorption of a second molecular layer with the functional groups oriented downwards and inserted between the upright standing functional groups of the underlying adsorbate layer. Due to the very open structure of the monolayer film, where the intermolecular distance between the surface-normal functional groups is substantially larger than their size, the driving force for such an insertion should be high. In contrast, for platforms without vertically attached groups, *i.e.*, the pure TATA molecules, no insertion is possible, in agreement with the complete absence of bilayer formation in the STM observations. Support for these ideas comes from X-ray diffraction studies of the **1a** crystal structure, which reveal a very similar interdigitated bilayer structure even for the bulk phase.[33] Most probably, the bimolecular stacking is caused by interactions between the π electrons in the aromatic functionalities. This is supported by the observation that substances with attached phenyl groups (**1a** and **2a**) exhibit a much smaller tendency to form bilayers than the substances with azobenzenyl groups (**1b** and **2b**). Furthermore, the substances with propyl side chains (**1a** and **1b**) form less ordered adlayers than those with octyl side chains (**2a** and **2b**).

Although a tendency towards bilayer formation may well be a general phenomenon in open self-assembled layers with well-separated groups, it presents a serious problem for the preparation of functional adlayers, in which a defined orientation of the attached functions (typically away from the metal surface) is desired. Partial bilayer formation limits the accessibility of the functional units to species in the adjacent gas or solution phase and results in a heterogeneous surface with locally different behavior. We therefore systematically studied the influence of the preparation conditions on the structural properties for the case of **2b** adlayers (Fig. 7), aiming to minimize the bilayer surface coverage and, if possible, to prepare a pure monolayer phase. In particular, the **2b** concentrations in the solutions used for the self-assembly were varied between 1×10^{-3} and 5×10^{-7} M, the immersion times between 30 min and 48 h, and the temperatures of the solutions between room temperature and 80 °C. For high TATA concentrations, long immersion times and room temperature, the formation of an almost complete bilayer with only a few small monolayer domains (dark areas) was observed (Fig. 7a). In contrast, shorter immersion times and lower concentrations resulted in surfaces only partially covered by bilayer islands (Fig. 7b). Further reduction of the bilayer coverage could be achieved by self-assembly at elevated temperatures. However, even for extreme preparation conditions (a **2b** concentration in the solution corresponding

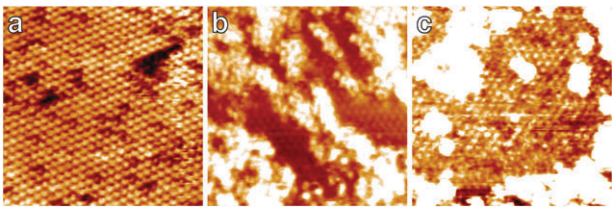

Fig. 7 Influence of the preparation conditions on the morphology of **2b** adlayers (30×30 nm^2). The adlayers were formed by self-assembly (a) for 22.5 h and (b) for 1 h in 10^{-4} M solution at room temperature and (c) for 30 min in 10^{-6} M solution at 80 °C.

to only ≈5 ML and a temperature of 80 °C), the presence of bilayer islands was still observed (Fig. 7c). In addition, no significant influence of the solvent species (dichloromethane, or toluene) on the bilayer formation was observed. These findings are in agreement with the trends expected for **2b** adsorption and again support the assignment of these structures to coadsorbed, second layer TATA. Furthermore, they do not only demonstrate that the TATA platform is strongly adsorbed on the Au substrate, but also indicate surprisingly strong intermolecular interactions between the first and second molecular layer of the functionalized molecules.

While for phenyl- or azobenzyl-functionalized platforms complete suppression of bilayer formation could not be achieved, almost perfect monolayer films could be prepared for TATA molecules to which different types of azobenzene derivatives with cyano, iodo, or dimethyl head groups (substances **2c**, **2d**, and **1e**) were attached (Fig. 5c, f, g and 8). For all adlayers of these molecules, bilayer coverages of <10% were found (brighter spots in the images). Under optimum conditions (especially for **2d** adlayers) large, highly-ordered hexagonal domains with diameters up to 200 nm were observed, which were completely free of bilayer aggregates (Fig. 8b, the small dark areas at the right-hand side of the image are pits in the Au substrate), indicating that for suitably functionalized TATA molecules the formation of well-defined, highly ordered adlayers is possible.

Apparently, the introduction of polar or bulky head groups significantly reduces the tendency towards bilayer formation. Possible explanations for this considerable difference to adlayers of the substances without these head group are steric blocking effects by the head groups (especially for the dimethyl derivative **1e**) as well as repulsive electrostatic interactions (the cyano and the iodo groups are electron withdrawing groups). These may destabilize the interdigitated stacking as well as contribute to a kinetic barrier for bilayer formation by impeding interpenetration of the functional group into the outer, open part of the monolayer film (whose outermost section carries the same head groups).

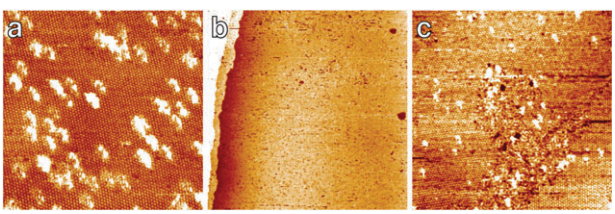

Fig. 8 Large-scale STM images of (a) a **2c** adlayer (80×80 nm^2), and (b, c) of a **2d** adlayer ((b) 200×200 nm^2, (c) 100×100 nm^2).

4. Conclusions

We have presented systematic structural studies of self-assembled molecular layers based on vertically functionalized triazatriangulenium platforms, demonstrating the general applicability and variability of our previously introduced, novel approach for the formation of functional molecular nanostructures.[28] As shown now for a variety of different molecules exhibiting different functional units with various head groups as well as with two types of side chains, structurally highly defined adlayers can be formed whose intermolecular spacing is solely determined by the adsorbed TATA platform rather than by packing of the vertically oriented functional groups. This affords the preparation of functionalized surfaces with attached freestanding molecular functions, that possess excellent stability under a broad range of conditions. Due to their open architecture, these molecular films exhibit a tendency towards bilayer formation, which can be surprisingly pronounced and may present an obstacle for applications of these functional adlayers that require a well-defined interface with the adjacent gas or liquid phase. However, bilayer formation may be completely suppressed by suitably derivatized adlayers, as shown here for the case of attached azobenzene functions with cyano, iodo, or dimethyl head groups.

Acknowledgements

We gratefully acknowledge financial support from the Deutsche Forschungsgemeinschaft *via* Son-der-for-schungs-be-reich 677 "Funktionen durch Schalten".

References

1 V. Balzani, A. Credi and M. Venturi, *ChemPhysChem*, 2008, **9**, 202–220.
2 T. Kondo and K. Uosaki, *J. Photochem. Photobiol., C*, 2007, **8**, 1–17.
3 J. C. Love, L. A. Estroff, J. K. Kriebel, R. G. Nuzzo and G. M. Whitesides, *Chem. Rev.*, 2005, **105**, 1103–1169.
4 F. Schreiber, *Prog. Surf. Sci.*, 2000, **65**, 151–257.
5 K. Tamada, H. Akiyama and T. X. Wei, *Langmuir*, 2002, **18**, 5239–5246.
6 K. Tamada, H. Akiyama, T.-X. Wei and S.-A. Kim, *Langmuir*, 2003, **19**, 2306–2312.
7 M. J. Comstock, N. Levy, A. Kirakosian, J. Cho, F. Lauterwasser, J. H. Harvey, D. A. Strubbe, J. M. J. Fréchet, D. Trauner, S. G. Louie and M. F. Crommie, *Phys. Rev. Lett.*, 2007, **99**, 038301.
8 H. B. Shao, D. Y. Li and J. S. Tu, *Chin. Chem. Lett.*, 1999, **10**, 145–146.
9 E. Jeoung and V. M. Rotello, *J. Supramol. Chem.*, 2002, **2**, 53–55.
10 S. Yasuda, T. Nakamura, M. Matsumoto and H. Shigekawa, *J. Am. Chem. Soc.*, 2003, **125**, 16430–16433.
11 S. D. Evans, S. R. Johnson, H. Ringsdorf, L. M. Williams and H. Wolf, *Langmuir*, 1998, **14**, 6436–6440.
12 H.-Z. Yu, J. W. Zhao, Y. Q. Wang, S. M. Cai and Z. F. Liu, *J. Electroanal. Chem.*, 1997, **438**, 221–224.
13 A. S. Kumar, T. Ye, T. Takami, B.-C. Yu, A.-K. Flatt, J. M. Tour and P. S. Weiss, *Nano Lett.*, 2008, **8**, 1644–1648.
14 P. S. Weiss, *Acc. Chem. Res.*, 2008, **41**, 1772–1781.
15 H. Akiyama, K. Tamada, J. 'i. Nagasawa, K. Abe and T. Tamaki, *J. Phys. Chem. B*, 2003, **107**, 130–135.

16 A. Manna, P.-L. Chen, H. Akiyama, T.-X. Wei, K. Tamada and W. Knoll, *Chem. Mater*., 2003, **15**, 20–28.
17 M. Onoue, M. R. Han, E. Ito and M. Hara, *Surf. Sci*., 2006, **600**, 3999–4003.
18 M. Ito, T. X. Wei, P.-L. Chen, H. Akiyama, M. Matsumoto, K. Tamada and Y. Yamamoto, *J. Mater. Chem*., 2005, **15**, 478–483.
19 G. Pace, V. Ferri, C. Grave, M. Elbing, C. von Hänisch, M. Zharnikov, M. Mayor, M. A. Rampi and P. Samorí, *Proc. Natl. Acad. Sci. U. S. A*., 2007, **104**, 9937–9942.
20 V. Ferri, M. Elbing, G. Pace, M. D. Dickey, M. Zharnikov, P. Samori, M. Mayor and M. A. Rampi, *Angew. Chem*., 2008, **120**, 3336.
21 T. Kondo, T. Kanai and K. Uosaki, *Langmuir*, 2001, **17**, 6317–6324.
22 Q. Li, A. V. Rukavishnikov, P. A. Petukhov, T. O. Zaikova, C. Jin and J. F. W. Keana, *J. Org. Chem*., 2003, **68**, 4862–4869.
23 T. Kitagawa, Y. Idomoto, H. Matsubara, D. Hobara, T. Kakiuchi, T. Okazaki and K. Komatsu, *J. Org. Chem*., 2006, **71**, 41362–1369.
24 S. Katano, Y. Kim, H. Matsubara, T. Kitagawa and M. Kawai, *J. Am. Chem. Soc*., 2007, **129**, 2511–2515.
25 T. Sakata, S. Maruyama, A. Ueda, H. Otsuka and Y. Miyahara, *Langmuir*, 2007, **23**, 2269–2272.
26 S. De Feyter and F. C. De Schryver, *Top. Curr. Chem*., 2005, **258**, 205–255.
27 V. Kriegisch and C. Lambert, *Top. Curr. Chem*., 2005, **258**, 257–313.
28 B. Baisch, D. Raffa, U. Jung, O. Magnussen, C. Nicolas, J. Lacour, J. Kubitschke and R. Herges, *J. Am. Chem. Soc*., 2009, **131**, 442–443.
29 C. Schönenberger, J. A. M. Sondag-Houethorst, J. Jorritsma and L. G. J. Fokkink, *Langmuir*, 1994, **10**, 611–614.
30 C. Wöll, S. Chiang, R. J. Wilson and P. H. Lippel, *Phys. Rev. B: Condens. Matter*, 1989, **39**, 7988–7991.
31 J. V. Barth, H. Brune, G. Ertl and R. J. Behm, *Phys. Rev. B: Condens. Matter*, 1990, **42**, 9307–9318.
32 O. Filinova, U. Jung, J. Kubitschke, R. Herges and O. Magnussen, unpublished.
33 C. Naether and R. Herges, unpublished.